Photoassociation Spectroscopy of Cold He(2³S) Atoms

N. Herschbach, P. J. J. Tol, W. Vassen, and W. Hogervorst

Department of Physics and Astronomy, Vrije Universiteit, De Boelelaan 1081, 1081 HV Amsterdam, The Netherlands

G. Woestenenk, J. W. Thomsen, P. van der Straten, and A. Niehaus

Debye Institute, Department of Atomic and Interface Physics, Utrecht University, P.O. Box 80.000,
3508 TA Utrecht, The Netherlands

We observe vibrational states by photoassociation spectroscopy of cold He(2³S) atoms. Photoassociation resonances are detected as peaks in the Penning ionization rate over a frequency range of 20 GHz below the atomic $2\,^3S_1$-$2\,^3P_2$ transition frequency. We have observed three vibrational series, of which two can be identified. A possible mechanism to explain the observed increase of the Penning ionization rate is discussed.

PACS numbers: 33.80.Eh, 32.80.Pj, 33.20.Tp

Photoassociation spectroscopy of cold atoms is a new and powerful technique to investigate long-range interactions between atoms [1,2]. Experiments in alkali-atom traps have revealed precise information on the long-range part of molecular potentials. This has resulted in the precise determination of *s*-wave scattering lengths for these systems, of high interest for studies of Bose-Einstein condensation in dilute trapped gases [3–5]. In these experiments a probe laser beam is sent through a cloud of cold atoms in a trap and the trap loss as a function of the laser frequency is detected. When the laser frequency is tuned to a photoassociative resonance, trap losses increase through the process of radiative escape or the formation of molecules, which are not trapped [2]. In some cases the excited molecules can also be photoionized by absorption of a second photon and the produced ions can be detected with high efficiency [1].

In view of this success it is obvious that application of the same method to cold rare gas metastables is of great value. Especially in the case of metastable He(2³S) atoms (He*), the detailed information that can be obtained on the long-range interactions of collision systems in ground and photoexcited states is of fundamental interest. Metastable rare gas systems differ from alkali systems mainly by the possibility of Penning ionization occurring at small internuclear distances. A molecule formed by photoassociation would contain an internal energy of 40 eV and its lifetime due to Penning ionization is expected to be short compared with a vibrational period, thereby excluding photoassociation spectroscopy for this system. For He(2³S) atoms, close collisions in the molecular $^1\Sigma_g^+$ or $^3\Sigma_g^+$ potentials have ionization probability close to unity [6], while for the $^5\Sigma_g^+$ potential the ionization probability is reduced by orders of magnitude [7] due to the total spin conservation selection rule. An ionization rate constant of 1.3×10^{-10} cm³/s in laser-cooled unpolarized He* atomic clouds [8] is attributed to these close collisions. It is to be expected that, for the molecular potentials

relevant for the photoassociation process, i.e., potentials that asymptotically belong to He(2³S)-He(2³P), the situation at small internuclear distances is equivalent: the singlet and triplet states decay with high probability, while the quintet states are stable. However, the fine-structure interaction implies the possibility of spin mixing at large distances. It is thus an open question how this mixing affects the formation and detection of photoassociated molecules. An earlier measurement of the ion rate as a function of the detuning did not show any vibrational resonances [9]. However, this measurement was aimed at a determination of the general shape of the ion rate curve and does not exclude the existence of such resonances due to insufficient statistics. In this paper we demonstrate that photoassociation spectroscopy is indeed possible on the He(2³S)-He(2³P) system.

To study photoassociation of He* below the $2\,^3S$-$2\,^3P_2$ asymptote, experiments have been carried out in Amsterdam and Utrecht using two different setups. Although the techniques used in both setups are similar, the two experiments focus on different aspects of the photoassociation process. In the Amsterdam experiment the dependence of the rate constant for ionization on the probe laser detuning is measured over 2 GHz around resonance, whereas in the Utrecht experiment photoassociation at larger detunings is studied. In principle, the effects of the probe laser on the cloud of cold atoms should be small, such that the detected signal is directly proportional to the rate of photoassociation. However, at high laser intensity the probe laser will always perturb the cloud close to resonance. In the case of He* this is a large effect due to its small atomic mass.

Both experimental setups use a cooled dc-discharge source of He* atoms. The He* atoms are decelerated with a Zeeman slowing technique and loaded into a magneto-optical trap (MOT). In the Utrecht experiment typically 5×10^6 atoms are trapped in a ~1 mm diam cloud. In Amsterdam the MOT contains typically 1×10^9 atoms [8]. In both experiments the temperature is ~1 mK and the

atom density around 5×10^9 cm^{-3}. The probe lasers are DBR (distributed Bragg reflector) diode lasers used free running in Utrecht, whereas in Amsterdam an extended cavity and frequency locking to a Fabry-Perot interferometer (FPI) are used. Relative frequency calibration is obtained from FPI markers and saturation spectroscopy in an rf-discharge cell yields an absolute frequency reference. Positive ions produced by Penning ionization are detected with a microchannel plate (MCP) detector at negative high voltage, whereas He* atoms released from the trap can be measured with a second MCP detector at ground potential. This enables time-of-flight determination of temperatures as well as measurement of fast neutral atoms escaping from the trap (radiative escape).

To measure the rate constant for ionization at relatively small detunings the experiment in Amsterdam is performed in a pulsed way such that the probe laser always sees an atomic cloud with the same characteristics. The probe laser and the trapping laser are switched with acousto-optic modulators. The MOT is loaded for 0.1 s and then switched off for 130 μs. During this trap-off time interval the probe laser is switched on for 60 μs and the ion current on an MCP is collected using a gated boxcar averager. Repetition rates below 10 Hz are necessary to ensure equilibration of the MOT before the next cycle. It turned out that the damping time constant of the MOT, around 10 ms in this case, is the relevant time scale to prevent cumulative effects from successive probe laser pulses, as observed with a video camera from the fluorescence of the trap. The intensity of the probe laser is about 14 mW/cm^2 (≈ 90 I_{sat}, $I_{sat} = 0.16$ mW/cm^2 being the saturation intensity). At higher intensities perturbation of the atomic cloud by the probe laser cannot be neglected around the atomic resonance. About 10 spectra were added to average out possible instabilities of the MOT. The calibration of the measured ion currents was done with respect to the MOT values previously calibrated [8].

The resulting rate constant for ionization is plotted on a logarithmic scale as a function of probe laser detuning in Fig. 1. Its accuracy is estimated to be better than 50%. The contribution of Penning ionization of background molecules to the measured ion currents is estimated to be smaller than 9×10^{-11} cm^3/s. The peaks in this curve, which are attributed to photoassociation resonances, are clearly visible. Choosing circular instead of linear polarization for the probe beam did not produce a significant difference in the spectrum. The peak structure became slightly more pronounced only when the magnet of the MOT was switched off, thus removing Zeeman broadening by the trap field. To determine the peak positions a steeply increasing but smooth curve is subtracted such that fitting could be done against a constant background. Peak positions are numbered and collected in Table I and indicated in Fig. 1.

The blue detuning part of the spectrum is interesting for the effect of optical shielding. Although our experimental conditions are similar to those in Xe*, where for blue
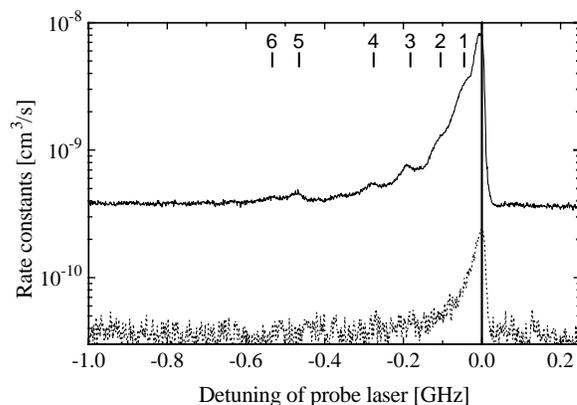

FIG. 1. Rate constants for ionization (solid line) and for radiative escape (dashed line). Both are measured with circularly polarized light. The radiative escape signal for $\Delta < -0.25$ GHz and $\Delta > 0.020$ GHz is a constant background of slow atoms released during the trapping phase against which the signal of the faster atoms is measured.

detuning a factor of 8 suppression of Penning ionization was observed [10], the ion signal in our case did not decrease below the level of S-S collisions (see Fig. 1).

In the Utrecht experiment photoassociation resonances up to detunings of -20 GHz are observed. The measurement is pulsed by modulating the trapping laser frequency. During the trapping phase the MOT laser operates at the trapping frequency and during the probe phase at a detuning of -600 MHz, which is sufficiently large to avoid enhancement of the ionization by the trapping laser. The repetition rate is 25 kHz and the duty cycle 50%, which was chosen such that the MOT does not expand appreciably during the probe phase. A gate to the counter is opened only in the probing phase, so only ions produced by the probe laser are measured together with ions produced in the probe phase by collisions with the background gas or He* atoms. To verify the stability of the MOT, the ion signal in the trap phase is monitored. A typical scan takes 100 s and for the spectrum a few scans are summed. In Fig. 2 two typical spectra using circularly polarized light with different saturation parameters are shown. The dotted line indicates the region where the MOT is perturbed by the probe laser. A structure of pronounced peaks overlaps the overall trend of ionization earlier observed by Mastwijk et al. [9]. The width of the peaks is in the order of 10 MHz for low intensities and increases with increasing intensity. Peaks up to a frequency of -21 GHz were measured and are collected in Table I. For the largest detunings the intensity of the probe laser is 2.1×10^5 I_{sat}, and then the probe laser perturbs the MOT already at a detuning of -5 GHz. The positions of the peaks found in both experiments agree within their uncertainty.

Photoassociation can also be observed by detecting trap loss via radiative decay and He* atoms are favorable in this respect as they can directly be detected with an MCP. The results for small detunings are shown in Fig. 1 as well, where the rate constant can be compared on an absolute

TABLE I. Red detunings Δ of the probe laser from the $2\,^3P_2$ atomic resonance at which photoassociation peaks are observed. The peaks are labeled from small to large detunings and, if possible, a tentative assignment is made. Peak positions $n = 1-6$ are measured in Amsterdam (uncertainty 3 MHz), 2–25 in Utrecht (uncertainty 20 MHz). Very weak peaks are given in parentheses.

n	Δ (GHz)	Ser.	n	Δ (GHz)	Ser.	n	Δ (GHz)	Ser.
1	0.045	⋯	10	1.77	1	18	6.85	3
2	0.105	0.11	2	11	1.91	⋯	19	7.26	2
3	0.182	0.19	⋯	12	2.27	3	20	8.80	1
4	0.275	0.27	2	13	2.43	2	(21)	10.73	3
5	0.465	0.45	1	14	3.20	1	(22)	11.43	2
6	0.533	0.50	3	15	4.07	3	23	13.67	1
7	⋯	0.59	2	16	4.32	2	(24)	20.11	⋯
8	⋯	0.93	1	17	5.45	1	(25)	21.01	⋯
9	⋯	1.20	2,3						

scale with the rate constant for Penning ionization. The behavior of both signals is comparable but in the radiative decay signal no pronounced peaks can be resolved. This is probably due to the poorer signal-to-noise ratio resulting from a 40 times smaller escape rate compared to the ionization rate and a small detection fraction. From the time the metastables take to reach the MCP we can deduce that 75% of these atoms are produced with high velocities in the range of 650 to 2500 m/s independent of the detuning of the laser. We can conclude that radiative decay contributes at most 2.5% to the total loss rate constant at these detunings.

To interpret the peak structure in the ion rate, we have carried out an analysis of the peak positions. The peak separation increases with increasing detuning from atomic resonance, which is a clear indication of a vibrational spectrum. Identification of the different peaks is more complicated compared to the alkali systems, since there is no hyperfine interaction, which often causes structures that indicate the symmetry of the state [11]. Furthermore, the temperature of the sample is well below the limit for pure s-wave scattering, and there is no rotational progression
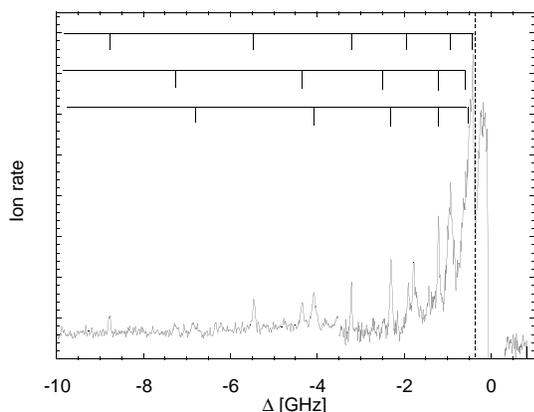

FIG. 2. Photoassociation spectrum of He* as a function of the detuning Δ of the probe laser. For the left side of the spectrum (from -10 to -3.5 GHz) the probe laser intensity is $1.2 \times 10^5 I_{\text{sat}}$ and for the right side (from -3.5 to 0 GHz) $7.5 \times 10^4 I_{\text{sat}}$. The assignment of the states to vibrational series is shown on top.

visible. Therefore the separation between the peaks, and to a lesser degree the strength and width of the peaks, is the only information that can be used to identify a series of vibrational peaks.

In a first attempt to identify the different vibrational series, we have used the LeRoy and Bernstein analysis for the positions of the vibrational states in a long-range C_n/R^n potential [12,13]. For the $2\,^3S-2\,^3P$ asymptote the long-range potential is determined by the dipole-dipole interaction C_3/R^3, where C_3 is proportional to the lifetime τ of the excited $2\,^3P$ state. In the absence of the fine structure [Hund's case (a)] there are two sets of attractive potentials, namely $^{1,3,5}\Sigma_g$ and $^{1,3,5}\Pi_u$ with $C_3 = -12.80$ and -6.40 a.u., respectively. However, due to the fine-structure interaction these potentials are strongly mixed and the resulting C_3 coefficients depend on the molecular symmetry for Hund's case (c). We have fitted the LeRoy-Bernstein formula to the peaks which form a vibrational progression. We find three series with $C_3 = -8.35$, -7.62, and -8.00 a.u., respectively. The assignment of the peaks to a particular vibrational series is indicated in Table I.

To analyze the spectrum further we have calculated the long-range Hund's case (c) potentials connected to the $2\,^3S-2\,^3P$ asymptote including fine-structure interaction, similar to the Movre-Pichler analysis [14] for the alkali systems. The resulting potential curves are shown in Fig. 3. There are in total 34 potentials, of which 10 are both attractive and connected to the $2\,^3S-2\,^3P_2$ asymptote. Because of avoided crossings between potential curves of the same symmetry connected to different asymptotes the potential can be approximated by C_3/R^3 with a fixed C_3 coefficient only at very long range ($>1000a_0$) and intermediate range [$(20-100)a_0$]. Since we probe vibrational states with outer turning point $(100-500)a_0$, the C_3 coefficients we found above are only average values, which depend on the range of detunings for the states included in the fitting procedure.

In order to calculate the vibrational states in the Hund's case (c) potentials, we have employed the method of accumulated phase, which was first described by Moerdijk *et al.* [15]. In this analysis the effect of the potential at
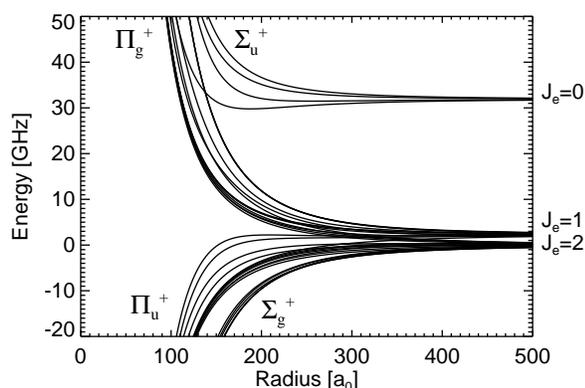
FIG. 3. Long-range potential curves for the Hund's case (c) states connected to the $2\,^3S-2\,^3P_{0,1,2}$ asymptotes. The mixing between the states is stretched out over a region from $(100-1000)a_0$.

small internuclear distance is reflected only in the total accumulated phase ϕ_0 at a matching distance R_0 and it is assumed that this phase is independent of the energy of the state. The wave function in the outer region is then integrated inwards for a certain energy using the known long-range potential. When the phase of the wave function in the outer region matches the phase ϕ_0 in the inner region, there is a resonance for that energy.

From our analysis we can conclude that energy positions of series 1 and 3 can be calculated using either a 0_g^+ or a 1_g potential. Since the two potentials are both connected at small range to $^{1,3,5}\Sigma_g$ and their long-range C_3 coefficients are nearly equal (-4.64 and -6.00 a.u., respectively), we cannot conclude with absolute certainty from the analysis, which potential belongs to which series. However, because the states in both potentials have large quintet character ($>80\%$), they will only weakly Penning ionize. Therefore it is to be expected that in these potentials vibrational states can be excited.

To give a physical reason why the excitation of vibrational states can lead to an increased ionization rate, we note that during the vibration of the molecule the system always crosses the region where the fine structure becomes comparable to the C_3/R^3 interaction. In this region singlet, triplet, and quintet states mix, and this mixing causes a transfer of amplitude of the quintet state, which is not ionized, to the singlet and triplet states, which can subsequently lead to ionization. This mixing, which depends on the binding energy of the state, is probably not very efficient, since otherwise no well-resolved vibrational structure would be observed. This possibly also accounts for the fact that below -20 GHz we are not able to observe vibrational states, if the excitation of these states is outside the region where the mixing takes place.

Finally, recent theoretical and experimental efforts to determine the absolute rate constant for Penning ionization led to an unsatisfactory disagreement between experimental and theoretical results [8,9,16,17]. In the theoretical

model [9] it is assumed that all potential curves contribute to the rate constant and an average is made over all states. Since we have identified the potentials, which are responsible for the vibrational structure, this can be taken into account, leading to a better agreement between theory and experiment.

To conclude, we have demonstrated that photoassociation spectroscopy of metastable triplet helium atoms is possible. This represents a significant improvement in the accessibility of the collisional interactions of this system, which might stimulate further investigations of the underlying long-range interaction potentials. In particular, a spectroscopic determination of the s-wave scattering length may become possible.

[1] P. D. Lett, P. S. Julienne, and W. D. Phillips, Annu. Rev. Phys. Chem. **46**, 423 (1995).

[2] W. C. Stwalley and H. Wang, J. Mol. Spectrosc. **195**, 194 (1999).

[3] E. Tiesinga, C. J. Williams, P. S. Julienne, K. M. Jones, P. D. Lett, and W. D. Phillips, J. Res. Natl. Inst. Stand. Technol. **101**, 505 (1996).

[4] E. R. I. Abraham, W. I. McAlexander, J. M. Gerton, R. G. Hulet, R. Côté, and A. Dalgarno, Phys. Rev. A **55**, R3299 (1997).

[5] J. R. Gardner, R. A. Cline, J. D. Miller, D. J. Heinzen, H. M. J. M. Boesten, and B. J. Verhaar, Phys. Rev. Lett. **74**, 3764 (1995).

[6] M. W. Müller, A. Merz, M.-W. Ruf, H. Hotop, W. Meyer, and M. Movre, Z. Phys. D **21**, 89 (1991).

[7] P. O. Fedichev, M. W. Reynolds, U. M. Rahmanov, and G. V. Shlyapnikov, Phys. Rev. A **53**, 1447 (1996).

[8] P. J. J. Tol, N. Herschbach, E. A. Hessels, W. Hogervorst, and W. Vassen, Phys. Rev. A **60**, R761 (1999).

[9] H. C. Mastwijk, J. W. Thomsen, P. van der Straten, and A. Niehaus, Phys. Rev. Lett. **80**, 5516 (1998).

[10] M. Walhout, U. Sterr, C. Orzel, M. Hoogerland, and S. L. Rolston, Phys. Rev. Lett. **74**, 506 (1995).

[11] P. D. Lett, K. Helmerson, W. D. Phillips, L. P. Ratliff, S. L. Rolston, and M. E. Wagshul, Phys. Rev. Lett. **71**, 2200 (1993).

[12] R. J. LeRoy and R. B. Bernstein, Chem. Phys. Lett. **5**, 42 (1970).

[13] W. C. Stwalley, Chem. Phys. Lett. **6**, 241 (1970).

[14] M. Movre and G. Pichler, J. Phys. B **10**, 2631 (1977).

[15] A. J. Moerdijk, W. C. Stwalley, R. G. Hulet, and B. J. Verhaar, Phys. Rev. Lett. **72**, 40 (1994).

[16] M. Kumakura and N. Morita, Phys. Rev. Lett. **82**, 2848 (1999).

[17] A. Browaeys, J. Poupard, A. Robert, S. Nowak, W. Rooijakkers, E. Arimondo, L. Marcassa, D. Boiron, C. I. Westbrook, and A. Aspect, Eur. Phys. J. D **8**, 199 (2000).